Signal Processing: Image Communication 74 (2019) 54–63

Contents lists available at ScienceDirect

Signal Processing: Image Communication

journal homepage: www.elsevier.com/locate/image

SSVD: Structural SVD-based image quality assessment

Azadeh Mansouri [a], Ahmad Mahmoudi-Aznaveh [b,*]

[a] Department of Engineering, Faculty of Electrical and Computer Engineering, Kharazmi University, Iran
[b] Cyberspace Research Institute, Shahid Beheshti University, Iran

ARTICLE INFO

Keywords:
Human visual system
Image quality assessment
Singular value decomposition(SVD)
SSVD

ABSTRACT

In the last decade, some impressive image quality metrics have been proposed; however, designing an image quality metric which predicts human judgments is still a challenging issue. It is due to the complexity of the human visual system. Singular value decomposition (SVD), as a useful tool, has been employed for evaluating the perceptual quality of visual information. The efficiency of the SVD-based image quality assessment (IQA) methods is related to its ability to extract the structural information of the viewing scene. In this paper, a new SVD-based IQA method is presented in which the structural information of the distorted image is evaluated based on its reflection on the original singular vector matrices. The experimental results show that the proposed algorithm can effectively evaluate the natural image quality in a consistent manner with the human visual perception.

1. Introduction

Designing a good image/video quality metric, with the rapid growth of digital communication, has become more important. A visual signal can be affected by a wide range of modifications/distortions. These alterations may occur during signal acquisition, transmission, compression, or other subsequent processes. Consequently, employing an appropriate quality metric is necessary in many visual processing applications such as image/video coding, information hiding and visual enhancement.

For evaluating the quality of the modified/distorted signals, the best judges are humans; hence, the most reliable and accurate quality assessment method is subjective evaluation. Admittedly, this kind of evaluation is very time consuming, cumbersome and thus cannot be applicable to real-world applications. As a result, many efforts have been made to design a method evaluating the distortions in accordance with the human visual system (HVS). Objective evaluation of visual quality considering the HVS is a difficult task, in that the HVS has a complicated and nonlinear behavior.

The simplest and widely used full reference image quality measurements are mean square error (MSE) and peak signal-to-noise ratio (PSNR). However, it is well-known that these two quality metrics are not reliable enough since they do not consider the image structure. Analysis of the human visual perception indicates that the structural information of the scene is one of the most important features which are effectively extracted by the HVS [1–3]. Based on this fact, in recent years many efforts have been made to assess the visual quality considering the structural information of the media [4–9]. In this paper, a new full reference image quality metric is proposed based on the image's structural similarity.

The basic idea of the proposed method is to employ the structural information using both the eigenvectors and eigenvalues in an effective manner. In fact, the structural information of the distorted image is evaluated based on its reflection on the original singular vector matrices. In other words, the deviation of the distorted image from the original one is calculated. In most of the SVD-based IQA methods, the SVD of the original and the distorted images are calculated independently and then compared. In this case, the dissimilarity of eigenvalues or eigenvectors cannot effectively evaluate the distortion amount. Our implementation of the SSVD is publicly available in order to facilitate reproducible research.[1]

In the next section, a review of the most important relevant methods is illustrated. In Section 3, the proposed method is explained. The experimental results and performance analysis are given in Section 4.

2. Previous work

In order to evaluate visual quality effectively, it is necessary to analyze the structure of natural images [1,2]. In spite of presenting impressive metrics, full reference image quality assessment is still a challenging issue. Universal quality index (UQI) [3] can be regarded as a pivotal scheme which has affected subsequent methods such as structural similarity index (SSIM) [2], multiscale SSIM (MS-SSIM) [10], complex wavelet SSIM (CW-SSIM) [11] and information content weighted SSIM (IW-SSIM) [12]. In [9], the information fidelity criterion (IFC) was

* Corresponding author.
E-mail addresses: a_mansouri@khu.ac.ir (A. Mansouri), a_mahmoudi@sbu.ac.ir (A. Mahmoudi-Aznaveh).

[1] http://faculties.sbu.ac.ir/~a_mahmoudi/Researches.htm.

https://doi.org/10.1016/j.image.2019.01.007
Received 31 May 2018; Received in revised form 17 January 2019; Accepted 17 January 2019
Available online 23 January 2019

introduced based on the information theory. This method was extended to the visual information fidelity (VIF) [13].

Feature similarity index (FSIM) employs gradient information to evaluate the perceived quality [5]. In this metric, phase congruency is utilized as well. Moreover, $FSIM_C$ – a generalization to color images – exploits chroma channels to estimate the local quality measure. The visual saliency-induced index (VSI), employs the visual saliency in addition to gradient similarity. VSI also simply incorporates the chroma channels M and N. Gradient magnitude similarity deviation (GMSD) [14] is another impressive gray level method in which edge information is employed. In superpixel-based similarity index (SPSIM), image gradient is also employed for evaluating structural degradations. Moreover, the reference and distorted images are segmented. The mean value of luminance and chrominance are compared in superpixels. The obtained features are then revised using regional gradient consistency and overall quality score is achieved using a weighting strategy employing the texture complexity [15].

Recently published Haar wavelet-based perceptual similarity index (HaarPSI) method employs high-frequency Haar wavelet coefficients to obtain local similarities. Its weight map is also derived from the response of a single Haar wavelet filter [16]. A generalization to color images was introduced which simply incorporates the chroma channels, I and Q.

In another approach toward image quality assessment, the singular value decomposition (SVD) is exploited. Shnayderman et al. utilized the difference between the singular values of the reference and the distorted images [17]. In this method, just the singular values (SVs) are employed for quality evaluation. Hence, the structural information is less effective in this scheme. In another scenario, some efforts have been conducted to utilize the eigenvectors to extract structural information for quality assessment [6–8,18–22].

In spite of presenting numerous image quality assessment methods, achieving a universal IQA method is still desirable and of course challenging. Using various features can reveal different aspect of HVS. Presenting different methods can be helpful for obtaining a near-ideal IQA metric.

In the following subsection, an in-depth theoretical analysis of SVD for visual quality assessment is presented. In particular, the effects of image distortion on singular values and vectors are explained.

2.1. SVD-based structural information analysis

In transform domain, the structural information of an input image is specified by basis images. In most frequency-domain transformations, such as DCT and DFT, the basis images are the same for all input images. In fact, changes in input images are captured by transform domain coefficients. Each coefficient shows the extent of contribution that the related basis image has made in constructing the whole input image.

$$F(u,v) = \langle B(u,v).A \rangle \tag{1}$$

In (1), $F(u, v)$ illustrates a transform domain coefficient achieved by the inner product of the related basis image ($B(u, v)$) and A as an input image. These coefficients demonstrate the structural similarity between the input image and the corresponding basis images. Therefore, further processing, such as quality evaluation, can be performed based on these coefficients. The various characteristics of transforms are related to these orthonormal basis images.

Using SVD, an image (A) can be decomposed into three matrices; a diagonal singular value (S) and two orthonormal eigenvector matrices (U and V).

$$A_{m\times n} = U_{m\times m} \times S_{m\times n} \times V^{\mathrm{T}}_{n\times n} \tag{2}$$

Let us consider U_i and V_i as the ith column of the left and right singular vector matrices (U and V). In this case, U_i and V_i are eigenvectors of AA^{T} and $A^{\mathrm{T}}A$ respectively. The ith singular value is illustrated as S_{i}. In addition, the following equations hold:

$$S_i = \left\| A.V_i \right\|, \quad i = 1, 2, 3, \ldots, m \tag{3}$$

$$U_i = \begin{cases} 0, & if\ S_i = 0 \\ A.V_i/S_i, & otherwise \end{cases} \tag{4}$$

The Eq. (2) can be rewritten as follows:

$$A_{m\times n} = \sum_{i=1}^{k} U_i \times S_i \times V_i^T, \quad k = \min(m, n) \tag{5}$$

To put it more simply, $U_i \times V_{\mathrm{i}}^{\mathrm{T}}$ can be regarded as the ith basis image (eigenimage) of the original input and S_i is its contribution factor to construct the whole image [23].

Although the basis images are constant for transforms such as DCT and DFT, they depend on the input image for SVD. Due to this fact, the structural information of the image can be better shown by fewer numbers of these dependent basis images. As a result, the most important parts of the structural information lay in the first basis images. More detailed information is added by increasing the index, until the complete image is constructed.

In Fig. 1, different basis images summation weighted by singular values are illustrated. It can be seen that with a limited number of SVD-based basis images, the input image structure is formed while the last basis images include high frequency content which are not perceptible by HVS. In Fig. 2, the same summation, but without considering the effect of singular values are depicted. In contrast to conventional transforms, the SVD-based basis images contain the main structure of the employed image.

2.2. SVD-based quality metrics

In this subsection, a brief review of SVD-based quality metrics is presented. For evaluating the rate of distortion, in M-SVD [17] the comparison between the singular values of the original and the distorted blocks is performed and finally, the overall M-SVD is computed as the average of the absolute difference between the block's error and median parameter over all blocks. Regarding the aforementioned points, singular values show the brightness or weight of the basis images in constructing the entire image. Thus, this method neglects the role of structural information. Consequently, various methods have been proposed [6–8,18–22] to improve the estimated perceptual quality considering the effect of singular vectors.

As the first attempt in [6], instead of computing the singular values of the distorted image directly, these values are estimated based on the right eigenvectors of the reference image as illustrated in (6) which are called reflection coefficients. It can be easily seen that the reflection coefficients of the undistorted image are its singular values:

$$\begin{aligned} &\hat{S}_i = \left\| \hat{A}.V_i \right\|, \\ &RF = \sum_i \left| \hat{S}_i - S_i \right| w_i \end{aligned} \tag{6}$$

In Eq. (6), $\hat{S}_i$ represents the ith reflection coefficient of the distorted image while S_i is the ith reflection coefficient (singular value) of the reference image. As illustrated in (6) and (7), these differences are weighted based on the eigenvalues (i.e. the influence of the eigenvectors):

$$w_i = \frac{S_i}{\left(\sum_j S_j\right)^2} \tag{7}$$

The sum of weighted differences indicates the numerical quality factor which is termed as *reflection factor* (RF) [6].

In another approach, R-SVD [7] utilizes the structural information obtained from singular vector matrices. Since the original and the distorted images are not structurally very different, right singular vector of the original image is utilized in order to obtain $\hat{U}$ and $\hat{S}$. In other words, to extract the structural information, the distorted image is

Fig. 1. Different basis images summation weighted by singular values for an image of size 384 × 512, the display range of part d is adjusted for better visualization (a) from 1 to 384 (100% (original image)), (b) from 1 to 8 (first 2%) (c) from 1 to 38 (first 10%) (d) from 346 to 384 (last 10%).

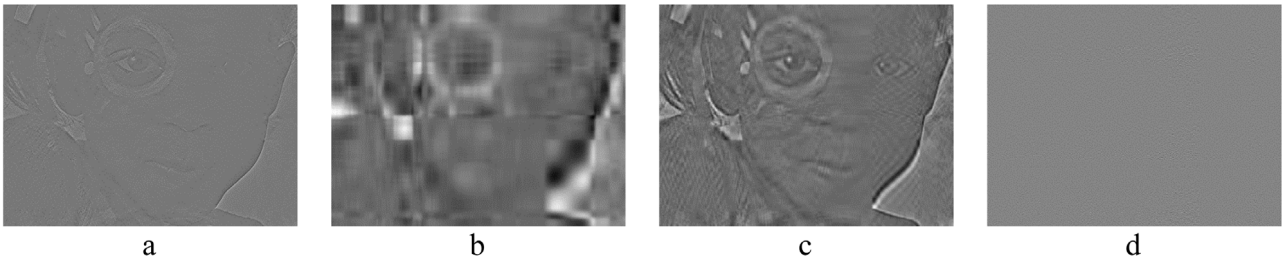

Fig. 2. Different basis images summation for an image of size 384 × 512, the display range of illustrated images are adjusted for better visualization, (a) from 1 to 384 (100%), (b) from 1 to 8 (first 2%) (c) from 1 to 38 (first 10%) (d) from 346 to 384 (last basis image).

decomposed into the basis images considering the reference image structure.

$$\hat{S}_i = \left\| \hat{\mathbf{A}}.\mathbf{V}_i \right\|, \quad i = 1, 2, 3, \ldots, m \tag{8}$$

$$\hat{\mathbf{U}}_i = \begin{cases} 0, & if\ \hat{S}_i = 0 \\ \hat{\mathbf{A}}.\mathbf{V}_i / \hat{S}_i, & otherwise \end{cases} \tag{9}$$

Then a referee matrix can be constructed as:

$$\hat{R}_{m\times n} = \hat{U}_{m\times m} \Lambda_{m\times n} V^T_{n\times n} \tag{10}$$

where Λ is a matrix with ones on the main diagonal and zeros elsewhere. In fact, the disparity of singular values of $\hat{R}$ (the referee matrix) from **ONE** shows the difference between the original and the distorted images.

The authors in [21] proposed to measure the difference between eigenvectors. The overall quality is determined by Minkowski summation. This idea is improved in [8] by employing M-SVD [17] as another feature indicating the perceived quality. In addition, support vector regression is utilized for estimating the overall quality based on SVD features. In [24,25], the combination of MSSIM, VIF and R-SVD is investigated. In [20], SVD is employed to decompose an image into two parts. Then, for each part a different quality factor is employed. In [18], a combined block-based approach utilizing R-SVD and M-SVD has been presented.

Most of the SVD-based methods have not effectively utilized the structural information represented by eigenvectors. In this case, their performances are not stable using different IQA datasets. In the proposed approach, both the structural degradation and luminance changes are captured.

3. Proposed method

Generally, the effect of any distortion can be broadly considered as the combination of two types of structural and luminance degradations. To evaluate the image quality, these two impairments are needed to be perceived. Since the human visual system is easily affected by structural degradation, an efficient quality metric has to effectively take the structural information into account. Still, the luminance information should not be neglected.

In this regard, a comprehensive metric should consider these two degradations. Referring to the aforementioned points, the structural information can generally be achieved through singular vectors. As it is expressed in Section 2.1, an image can be constructed through linear combination of the basis images. In fact, singular values (weights of the basis images) mainly show the luminance factor. In this paper, both singular values and vectors are exploited to effectively estimate the perceived visual quality. The structural and luminance degradations are estimated separately. The overall quality measure is a combination of these components. However, it should be noted that it is not feasible to separate the luminance and structural information completely due to their reciprocal effects.

First, the original and distorted images are divided into non-overlapping blocks of size $n \times n$. The quality of each block is measured separately. Finally, the quality metric of the entire image is obtained by averaging the computed local quality measures. The procedures to compute proposed method (SSVD) are depicted in Fig. 3. The details of the proposed method are as follows.

In [7], it is shown that the singular vectors alterations represent the structural degradations. The original and distorted blocks are considered as A and $\hat{A}$ respectively. Firstly, the SVD is just applied on the reference block. An estimate of the left singular vectors of the distorted block, $\hat{U}$, is achieved based on the right singular vectors of the original block (V) as mentioned in (9). The more similar the distorted block $\hat{A}$ to the original A is, the closer the value of $\hat{U}$ to U. As a result and based on SVD characteristics, for a perfect image it is expected that $U\hat{U}^T = I$. On this principle, the deviation of $U\hat{U}^T$ from identity matrix can be regarded as the structural deformation. In order to evaluate the similarity between $\hat{U}$ and U in a compact way, the singular values of $U\hat{U}^T$ is calculated. These singular values are called S_V and represent the structural impairment of $\hat{U}$ obtained based on the original V. In the same way, $\hat{V}$ can be constructed using original left singular vector (U) and the distorted block. S_U can be obtained in a similar way.

For each block, both these structural impairments are calculated. As a result, F^{SU} and F^{SV} are obtained through (11):

$$F^{SU} = \sqrt{\sum_{i=1}^{CPF} \left[(SU_i - 1)w_i\right]^2}, \qquad F^{SV} = \sqrt{\sum_{i=1}^{CPF} \left[(SV_i - 1)w_i\right]^2} \tag{11}$$

in which *CPF* indicates content-dependent threshold. CPF is exploited since the last nonzero singular values have a minor effect on quality

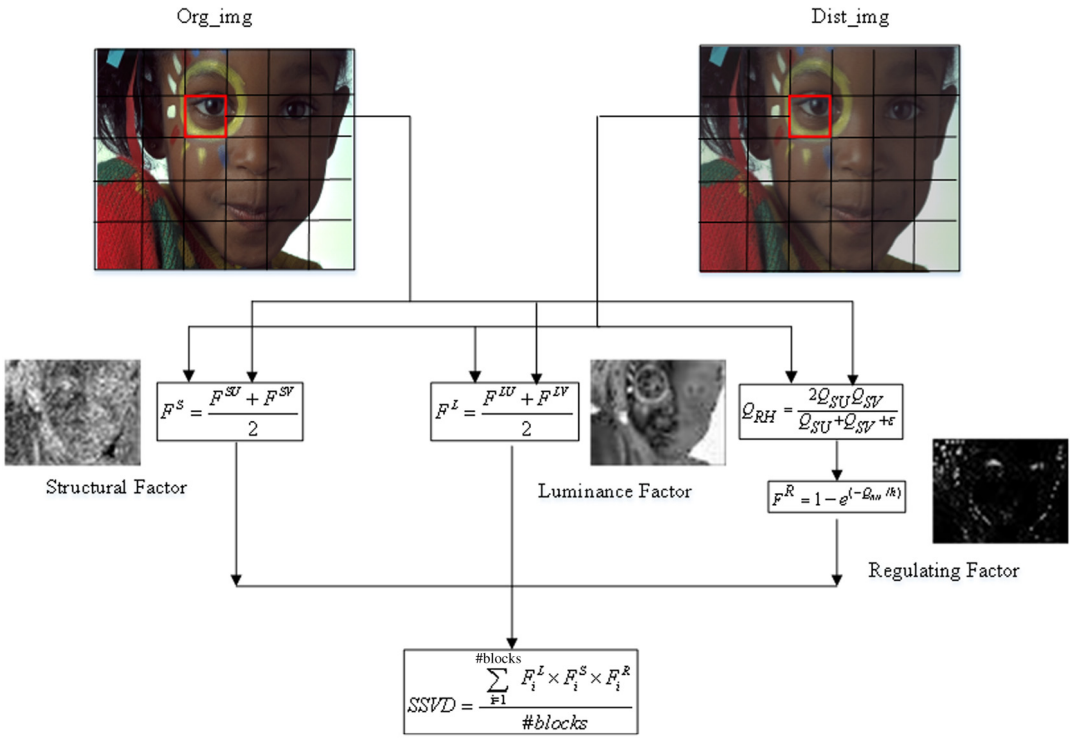

Fig. 3. Illustration for the SSVD metric.

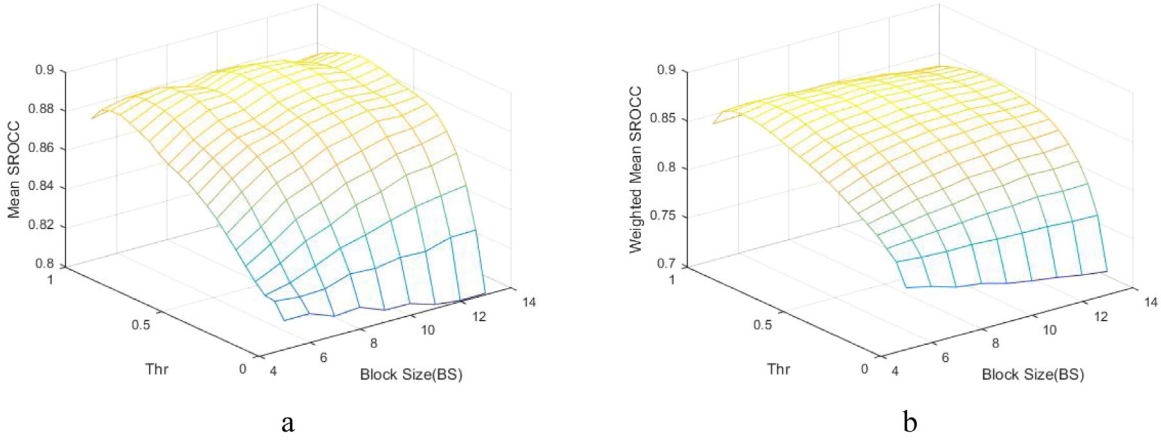

Fig. 4. The SROCC value as functions of *Thr* and block size (*BS*) (a) Mean SROCC (b) Weighted Mean of SROCC.

degradation as illustrated in Fig. 1. In other words, their effects are usually not detectable by HVS. Therefore, a content-dependent threshold called *CooPerative Factor (CPF)* is introduced in such a way that the following condition holds:

$$\frac{\sum_{i=1}^{CPF} \left|(S_i - \hat{S}_{Ui})\right| + \left|(S_i - \hat{S}_{Vi})\right|}{\sum_{i=1}^{NOS} \left|(S_i - \hat{S}_{Ui})\right| + \left|(S_i - \hat{S}_{Vi})\right|} = Thr \tag{12}$$

in which *NOS* indicates the number of nonzero singular values and *Thr* shows the rate of the cooperation considering the impressive values. In other words, incorporating these last non-important elements may degrade the objective results since these changes cannot be perceived by HVS.

Furthermore, w_i is a weighting factor demonstrating the relative importance of the original basis images:

$$w_i = S_i \Big/ \sum_{i=1}^{blk-size} S_i + C \tag{13}$$

As it is depicted in Figs. 1 and 2, the first basis images include structural information and the last ones contain details. As a case in point, the last 38(~10%) basis images mainly have a noise-like structure which is hardly perceptible. It should be noted that the singular values are sorted in ascending order and therefore the larger singular values are corresponded to more perceptually important basis images. In (13), the small constant $C \ll 1$ is included to avoid instability. The mean value of two factors indicates the block structural distortion.

$$F^S = \frac{F^{SU} + F^{SV}}{2} \tag{14}$$

To evaluate the luminance alterations, considering the changes in singular values of the original and distorted images is not effective. This is because the basis images of the distorted media may also be altered. Thus, in the proposed method the modified version of (*RF*) is exploited [6].

Here, both the left and right singular vector matrices are employed in order to provide $\hat{S}_U$ and $\hat{S}_V$ (Eq. (6)) for calculating F^{LU} and F^{LV}:

$$F^{LU} = \sqrt{\sum_{i=1}^{CPF} \left|(S_i - \hat{S}_{Ui})\right| w_i}, \qquad F^{LV} = \sqrt{\sum_{i=1}^{CPF} \left|(S_i - \hat{S}_{Vi})\right| w_i} \tag{15}$$

Subsequently, the mean value of two factors indicates the block luminance distortion as follows:

$$F^L = \frac{F^{LU} + F^{LV}}{2} \tag{16}$$

In addition, some distortions such as DC shift and contrast change do not degrade the structural information notably. However, these kinds of modifications may have a large effect on F^L as luminance degradation measure. Since the HVS is less sensitive to this group of alterations (DC shift and contrast change), we propose a regulating factor to alleviate the effect of these kinds of changes.

The fact is that these kinds of modifications are mostly considered as an acceptable quality in subjective scores since the most important part (structural information) is not changed. A regulating factor can adjust the objective results. Thus, this factor is introduced as follows:

$$Q_{SU} = \sqrt{\sum_{i=1}^{CPF} (Sd_i - \hat{S}_{Ui})^2}, \qquad Q_{SV} = \sqrt{\sum_{i=1}^{CPF} (Sd_i - \hat{S}_{Vi})^2}, \tag{17}$$

in which S_d, is the singular values of the distorted block. It should be noted that $\hat{S}_U$ and $\hat{S}_V$ are reflected coefficients which are obtained based on singular vectors of the original image as explained in (8). When the structure of the distorted block is close to the original block, the difference between these values and S_d is negligible.

In order to calculate the regulating parameter, the harmonic mean of these two values is calculated. The harmonic mean of a list of numbers tends to alleviate the impact of large numbers. In fact, it can better capture the effect of distortions which have a minor effect on structural information.

$$Q_{RH} = \frac{2Q_{SU}Q_{SV}}{Q_{SU} + Q_{SV} + \varepsilon} \tag{18}$$

Nevertheless, the calculated Q_{RH} has a non-linear effect on the perceived quality. Therefore, it is required to employ a nonlinear transformation:

$$F^R = 1 - e^{(-Q_{RH}/h)} \tag{19}$$

In (19), h is employed as a degree of adjustment. In our implementation h is considered as (4 × block size). When the distortion caused mostly by structural modifications, the Q_{RH} is noticeable. In this case, the resultant F^R is close to one. It means that the calculated F^L is reasonable and should remain relatively unchanged. On the other hand, in the case of luminance alterations with preserving structural information, Q_{RH} is negligible and the resultant F^R is used to alleviate the effect of the calculated F^L. Hence, the F^R parameter can regulate the effect of non-structural degradations.

Finally, the three calculated Structural Factor (F^S), Luminance Factor (F^L) and Regulating Factor (F^R) are combined to calculate the block perceived quality. The overall image distortion measure can be obtained as:

$$SSVD = \frac{\sum_{i=1}^{\#blocks} F_i^L \times F_i^S \times F_i^R}{\#blocks} \tag{20}$$

in which zero illustrates the best quality when the original and the distorted image are the same.

4. Performance analysis

The consistency of the proposed image quality metric with HVS is evaluated using large public image quality benchmarks including LIVE [2], TID2008 [26], TID2013 [27], CSIQ [28], MICT [29], VCL [30], IVC [31], WIQ [32] and IVL [33,34]. The mentioned datasets have different characteristics in the number of reference and distorted images, the distortion types, level of distortions and weather it contains single or multiple distortions.

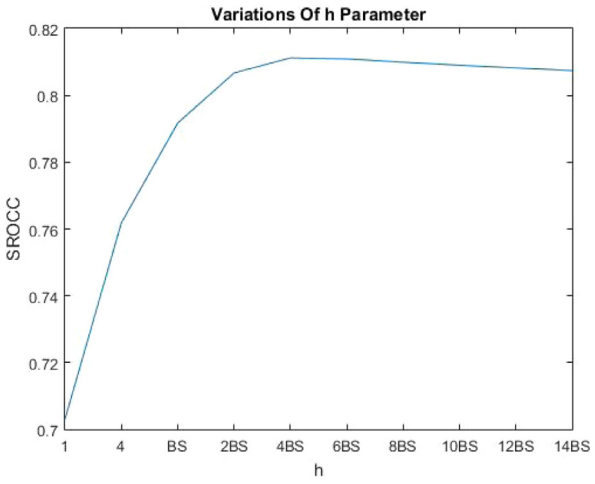

Fig. 5. The SROCC value as function of h on TID2103 dataset.

In order to evaluate the performance of the quality assessment methods four evaluation criteria are usually employed. The Spearman rank order correlation coefficient (SROCC) and the Kendall rank order correlation coefficient (KROCC) are the two correlation metrics which measure the monotonicity of the predictions. Both SROCC and KROCC only measure the rank of the quality scores. On the other hand, the Pearson linear correlation coefficient (PLCC) and the root mean squared error (RMSE) between subjective and objective scores are utilized in order to evaluate the prediction accuracy and consistency. PLCC and RMSE is computed after nonlinear mapping between subjective and objective scores provided by a logistic mapping function suggested in [4].

In the following, the experimental results will be given and explained. It should be noted that the proposed method requires three parameters as block size, threshold value(*Thr*) and *h*.

4.1. Parameter selection

In this subsection, *Thr*, *h* and block size (*BS*) as the three employed parameters are investigated considering their effects on the overall performance. The SROCC for all datasets is calculated based on different block sizes and *Thr* values. In Fig. 4, both the mean and the weighted mean of SROCCs are depicted. The results illustrate that the performance of the proposed method is not highly dependent on the block size. Conversely, the SROCC values are severely affected by the appropriate threshold value (*Thr*) selection.

Moreover, the effect of *h* values on SROCC has been inspected. As depicted in Fig. 5, 4 × BS can lead to an appropriate result. Since the amount of luminance change is highly related to the block size, the dependency of the *h* parameter to block size seems reasonable. In the following evaluations, the block size is considered as 9 and the threshold value (*Thr*) is set to 0.75.

The efficiency of the objective IQA metrics highly depends on using an appropriate scale. The image resolution and the viewing distance affect the "precisely right scale" which is usually difficult to be obtained [35]. In [35], an empirical method is suggested to obtain an appropriate scale which is adopted in many subsequent methods such as [5]. We also employed this method for downsampling in order to obtain the appropriate scale. Moreover, this preprocessing can approximate the low pass filter characteristics of the human visual system [36].

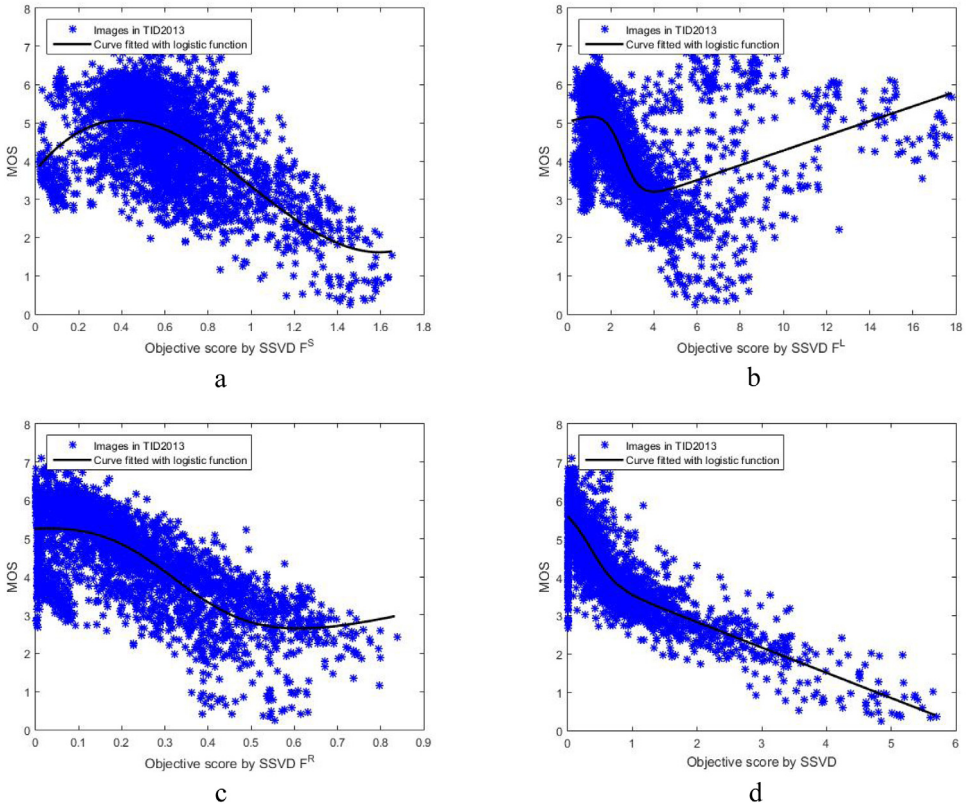

Fig. 6. Scatter plots of the subjective versus objective scores on TID2013 dataset. (a) F^S, (b) F^L, (c) F^R, (d) SSVD (proposed method).

4.2. Evaluation of the three contributing factors of SSVD

In this subsection, the effect of each factor on final quality score is investigated. In Fig. 6, the scatter plot of the subjective MOS versus objective scores on the TID2013 dataset are illustrated for each factor separately. The scatter plot of SSVD containing the three factors (F^S, F^L and F^R) clearly illustrates the effect of this combination.

4.3. Performance comparison on individual distortion types

In order to analyze the proposed method's ability to estimate image degradations caused by specific types of distortions, an experiment has been conducted. To save space, only SROCC scores are expressed. The performance of the proposed method is evaluated and compared with ten gray level image quality metrics including HaarPSI [16],GMSD [37] and FSIM [5].

In Table 1, the SROCC of the various distortion types are shown and the top results are highlighted in boldface. Table 1 clearly illustrates that the GMSD provides better results in individual type of the distortion and the proposed metric (SSVD) shows an acceptable performance in prediction scores. It should be noted that, good results on specific types of distortions do not guarantee the overall performance on a dataset with a diverse type of distortions. The full results of Table 2, also indicates that our proposed approach is less sensitive to the types of distortions and performs better on the whole dataset.

4.4. General performance comparison

In Fig. 7, the scatter plots of predicted quality scores against subjective scores for state of the art FR-IQA models and the proposed approach (SSVD) are depicted. The FR-IQA metrics are IW-SSIM, MAD, FSIM, GMSD, and HaarPSI. TID2013 is selected because of its diverse distortion types including twenty four types of distortions in five levels. Although all the results of the presented methods provide acceptable consistency with the subjective scores; it is clear that for the proposed method the sample points are better fitted around the curve. This can also be validated by comparing PLCC and RMSE values through Table 2,

In Table 2, the comparison between the most recent and effective image quality assessment methods and the proposed approach is illustrated. As it is mentioned, we make use of ten FR-IQA and ten image quality datasets in this evaluation.

The top results for each criterion including SROCC, KROCC, PROCC and RMSE are shown in boldface. In most of the datasets, including TID2013 and TID2008 with diverse types of distortions the proposed quality measure is well correlated in terms of accuracy and consistency. Moreover, for IVL database including single and multiple distortions named as SD-IVL and MD-IVL the superior results are achieved by the proposed SSVD method. In addition, the mean value and the weighted mean results are also illustrated. Considering the overall and distortion specific performance, the effectiveness of the proposed method can be concluded.

In order to evaluate the performance of competing methods, a series of statistical significance tests are also conducted. Two residuals between the nonlinearly mapped objective scores of two methods and the corresponding subjective scores are compared. The F-test has been mostly used to test the equality of variance of two sets of residuals. The F-test however assumes that the sets of residuals are independent. Since IQA methods are computed on the same datasets, the two sets of residuals may be correlated. As a result, the Pitman–Morgan test is employed to examine the equality of the variances. In this test, the Pearson correlation coefficient is used to consider the effect of correlation between two sets of residuals [38].

More complete information can be obtained by employing statistical significance test in which the results are illustrated in Fig. 8. In addition to LIVE and MICT, both TID2013 and TID2008 are chosen because of their diverse distortion types. Moreover, the IVL dataset including SD and the new MD version is evaluated in this test. The results clearly illustrate an acceptable performance of the proposed method

Table 1
Comparison of SROCC of IQA metrics for each distortion type in TID2013, AGN (Additive Gaussian noise), ANC (Additive noise in color components), SCN (Spatially correlated noise), MN (Masked noise), HFN (High frequency noise), IN (Impulse noise), QN (Quantization noise), GB (Gaussian blur), DEN (Image denoising), JPEG (JPEG compression), JP2K (JPEG2000 compression), JGTE (JPEG transmission errors), J2TE (JPEG2000 transmission errors), NEPN (Non eccentricity pattern noise), BLOCK (Local block-wise distortions of different intensity), MS (Mean shift (intensity shift), CTC (Contrast change), CCS (Change of color saturation), MGN (Multiplicative Gaussian noise), CN (Comfort noise), LCNI (Lossy compression of noisy images), ICQD (Image color quantization with dither), CHA (Chromatic aberrations), SSR (Sparse sampling and reconstruction), FF (Fat Fading), Lar (Locally Adaptive Resolution), GCD (Global Contrast Decrements).

		MSSIM	VIF	IWSSIM	SSIM	NQM	PSNR	IFC	FSIM	GMSD	HaarPSI	SSVD
TID2013	AGN	0.8646	0.8994	0.8438	0.8671	0.8171	0.9291	0.6612	0.8973	**0.9462**	0.9304	0.9221
	ANC	0.7730	0.8299	0.7515	0.7726	0.7403	**0.8981**	0.5352	0.8208	0.8684	0.8536	0.8289
	SCN	0.8544	0.8835	0.8167	0.8515	0.7880	0.9200	0.6601	0.8750	0.935	0.9199	**0.9369**
	MN	0.8073	0.845	0.802	0.7767	0.6852	**0.8323**	0.6932	0.7944	0.7075	0.7851	0.7325
	HFN	0.8604	0.8972	0.8553	0.8634	0.8700	0.9140	0.7406	0.8984	**0.9162**	0.9074	0.8995
	IN	0.7629	**0.8537**	0.7281	0.7503	0.7907	0.8968	0.6408	0.8072	0.7637	0.8447	0.7671
	QN	0.8706	0.7854	0.8468	0.8657	0.8261	0.8808	0.6282	0.8719	**0.9049**	0.8773	0.8572
	GB	0.9673	0.965	**0.9701**	0.9668	0.9005	0.9149	0.8907	0.9551	0.9113	0.9149	0.9499
	DEN	0.9268	0.8911	0.9152	0.9254	0.9195	0.9480	0.7779	0.9302	**0.9525**	0.945	0.9486
	JPEG	0.9265	0.9192	0.9187	0.92	0.8765	0.9189	0.8357	0.9324	**0.9507**	0.943	0.9318
	JP2K	0.9504	0.9516	0.9506	0.9468	0.9269	0.8840	0.9078	0.9577	0.9657	0.9675	**0.9688**
	JGTE	0.8475	0.8409	0.8388	**0.8493**	0.7321	0.7685	0.7425	0.8464	0.8403	0.849	0.8441
	J2TE	0.8889	0.8761	0.8656	0.8828	0.8068	0.8883	0.7769	0.8913	0.9136	0.9214	**0.9332**
	NEPN	0.7968	0.772	0.8011	0.7821	0.7463	0.6863	0.5737	0.7917	**0.814**	0.8104	0.8085
	Block	0.4801	0.5306	0.3717	0.572	0.0064	0.1552	0.2414	0.5489	**0.6625**	0.4601	0.4768
	MS	**0.7906**	0.6276	0.7833	0.7752	0.6092	0.7671	0.5522	0.7531	0.7351	0.7389	0.7507
	CTC	0.4634	**0.8386**	0.4593	0.3775	0.4623	0.4400	0.1798	0.4686	0.3235	0.462	0.4494
	CCS	0.4099	0.3099	**0.4196**	0.4141	0.1591	0.0766	0.4029	0.2748	0.2948	0.417	0.3562
	MGN	0.7786	0.8468	0.7728	0.7803	0.7727	**0.8905**	0.6143	0.8469	0.8886	0.8803	0.8600
	CN	0.8528	0.8946	0.8762	0.8566	0.8755	0.8411	0.816	0.9121	**0.9298**	0.9229	0.9263
	LCNI	0.9068	0.9204	0.9037	0.9057	0.9064	0.9145	0.818	0.9466	0.9629	0.9558	**0.9649**
	ICQD	0.8555	0.8414	0.8401	0.8542	0.8635	**0.9269**	0.6006	0.8760	0.9102	0.8958	0.8948
	CHA	0.8784	0.8848	0.8682	0.8775	0.8174	**0.8872**	0.821	0.8715	0.853	0.8723	0.8816
	SSR	0.9483	0.9353	0.9474	0.9461	0.9468	0.9042	0.8885	0.9565	0.9683	0.9642	**0.9700**
TID2008	AGN	0.8086	0.8797	0.7869	0.8107	0.7679	0.7347	0.5806	0.8566	**0.918**	0.9049	0.8955
	ANC	0.8054	0.8757	0.792	0.8029	0.7490	0.8546	0.546	0.8527	**0.8977**	0.8945	0.8208
	SCN	0.8209	0.8698	0.7714	0.8144	0.7720	0.7461	0.5958	0.8483	0.9132	0.9078	**0.9208**
	MN	0.8107	**0.8683**	0.8087	0.7795	0.7067	0.6120	0.6732	0.8021	0.7087	0.7919	0.7496
	HFN	0.8694	0.9075	0.8662	0.8729	0.9015	0.8042	0.7318	0.9093	**0.9189**	0.9172	0.9113
	IN	0.6907	0.8327	0.6464	0.6732	0.7616	**0.8596**	0.5345	0.7452	0.6611	0.7944	0.7005
	QN	0.8589	0.797	0.8177	0.8531	0.8209	0.7057	0.5857	0.8564	**0.8875**	0.8675	0.8609
	GB	0.9563	0.954	**0.9636**	0.9544	0.8846	0.7740	0.8559	0.9472	0.8968	0.9006	0.9351
	DEN	0.9582	0.9161	0.9473	0.953	0.9450	0.8352	0.7973	0.9603	**0.9752**	0.9712	0.9653
	JPEG	0.9322	0.9168	0.9184	0.9252	0.9075	0.7520	0.818	0.9279	**0.9525**	0.9399	0.9380
	JP2K	0.9700	0.9709	0.9738	0.9625	0.9532	0.6673	0.9437	0.9773	0.9795	0.9834	**0.9845**
	JGTE	0.8681	0.8585	0.8588	0.8678	0.7373	0.7208	0.7909	0.8708	0.8621	**0.8749**	0.8730
	J2TE	0.8606	0.8501	0.8203	0.8577	0.7262	0.7480	0.7301	0.8544	0.8825	0.8961	**0.9110**
	NEPN	0.7377	0.7619	0.7724	0.7107	0.6800	0.5945	**0.8418**	0.7491	0.7601	0.7926	0.7532
	Block	0.7546	0.8324	0.7623	0.8462	0.2348	0.8513	0.677	0.8492	**0.8967**	0.8029	0.8062
	MS	**0.7336**	0.5096	0.7067	0.7231	0.5245	0.5576	0.425	0.6720	0.6486	0.6598	0.6434
	CTC	0.6381	**0.8188**	0.6301	0.5246	0.6191	0.4459	0.1713	0.6481	0.4659	0.6358	0.6074
CSIQ	AGWN	0.9471	0.9575	0.938	0.8974	0.9384	0.9363	0.8431	0.9262	**0.9676**	0.9649	0.9474
	JPEG	0.9634	**0.9705**	0.9662	0.9546	0.9527	0.8881	0.8412	0.9654	0.9653	0.9702	0.9593
	JP2K	0.9683	0.9672	0.9683	0.9606	0.9631	0.9362	0.9252	0.9685	0.9718	**0.9792**	0.9692
	AGPN	0.9331	0.9511	0.9059	0.8922	0.9119	0.9339	0.8261	0.9234	0.9503	**0.9533**	0.9392
	GB	0.9711	0.9745	0.9782	0.9609	0.9584	0.9291	0.9527	0.9729	0.9713	**0.9783**	0.9713
	GCD	0.9526	0.9345	**0.9539**	0.7922	0.9479	0.8621	0.4873	0.9420	0.9039	0.9386	0.8690
LIVE	JP2K	0.9627	0.9696	0.9649	0.9614	0.9438	0.8943	0.9113	**0.9717**	0.9711	0.9699	0.9681
	JPEG	0.9810	0.9846	0.9808	0.9764	0.9644	0.8826	0.9468	0.9834	0.9782	**0.9848**	0.9805
	AWGN	0.9725	0.9858	0.9667	0.9694	**0.9862**	0.9849	0.9382	0.9652	0.9737	0.9801	0.9816
	GB	0.9561	0.9728	0.972	0.9517	0.8436	0.7882	0.9584	0.9708	0.9567	0.9682	0.9387
	FF	0.9462	**0.965**	0.9442	0.9556	0.8112	0.8898	0.9629	0.9499	0.9416	0.9546	0.9392
	AWGN	0.9398	**0.9688**	0.9405	0.9138	0.9595	0.9740	0.8743	0.9331	0.9444	0.9580	0.9545
VCL	BLU (GB)	0.9154	**0.9575**	0.9563	0.9046	0.9603	0.7791	0.9495	0.9420	0.9373	0.9523	0.9296
	J2K	0.9371	0.9499	**0.9515**	0.9353	0.9326	0.8519	0.8922	0.9484	0.9493	0.9498	0.9413
	JPEG	0.9334	0.9519	0.9425	0.9236	0.8999	0.6040	0.8306	0.9523	0.9501	**0.9538**	0.9537
MICT	JPEG	0.8618	0.9061	**0.9204**	0.8590	0.8893	0.2868	0.8928	0.8991	0.8235	0.8454	0.8857
	J2K	0.9377	0.9559	0.9549	0.9399	0.9073	0.8605	0.8103	**0.9566**	0.9369	0.9361	0.9414
IVC	JPEG	0.9225	0.9240	0.9468	0.9225	0.8532	0.6740	0.8538	**0.9554**	0.9461	0.9235	0.9508
	Blur	0.9033	0.9780	0.9604	0.8813	0.9516	0.6835	0.8286	0.9560	0.9077	0.9429	**0.9824**
	Lar	0.8561	0.8802	0.8960	0.8713	0.8394	0.6333	0.9090	0.8397	0.8622	0.8587	**0.9297**
	J2K	0.9031	0.9117	0.9263	0.9126	0.8334	0.7786	0.8963	**0.9408**	0.9337	0.9281	0.9194
IVL_S	noise	0.9569	0.9642	0.9439	0.9524	0.9199	0.9738	0.7553	0.9100	**0.9755**	0.9677	0.9617
	Jpeg	0.9134	0.9273	0.9243	0.9067	0.8948	0.8432	0.8293	0.9238	0.9272	0.9270	**0.9330**
IVL_M	Blur_JPEG	0.8242	0.8589	**0.8778**	0.7955	0.7655	0.6572	0.8630	0.8608	0.8372	0.8473	0.8736
	Noise_JPEG	0.8378	0.9278	0.8713	0.8085	0.8970	0.5841	0.7275	0.8931	0.8860	0.9155	**0.9334**
Hit count		2	8	7	1	1	6	1	4	17	6	12

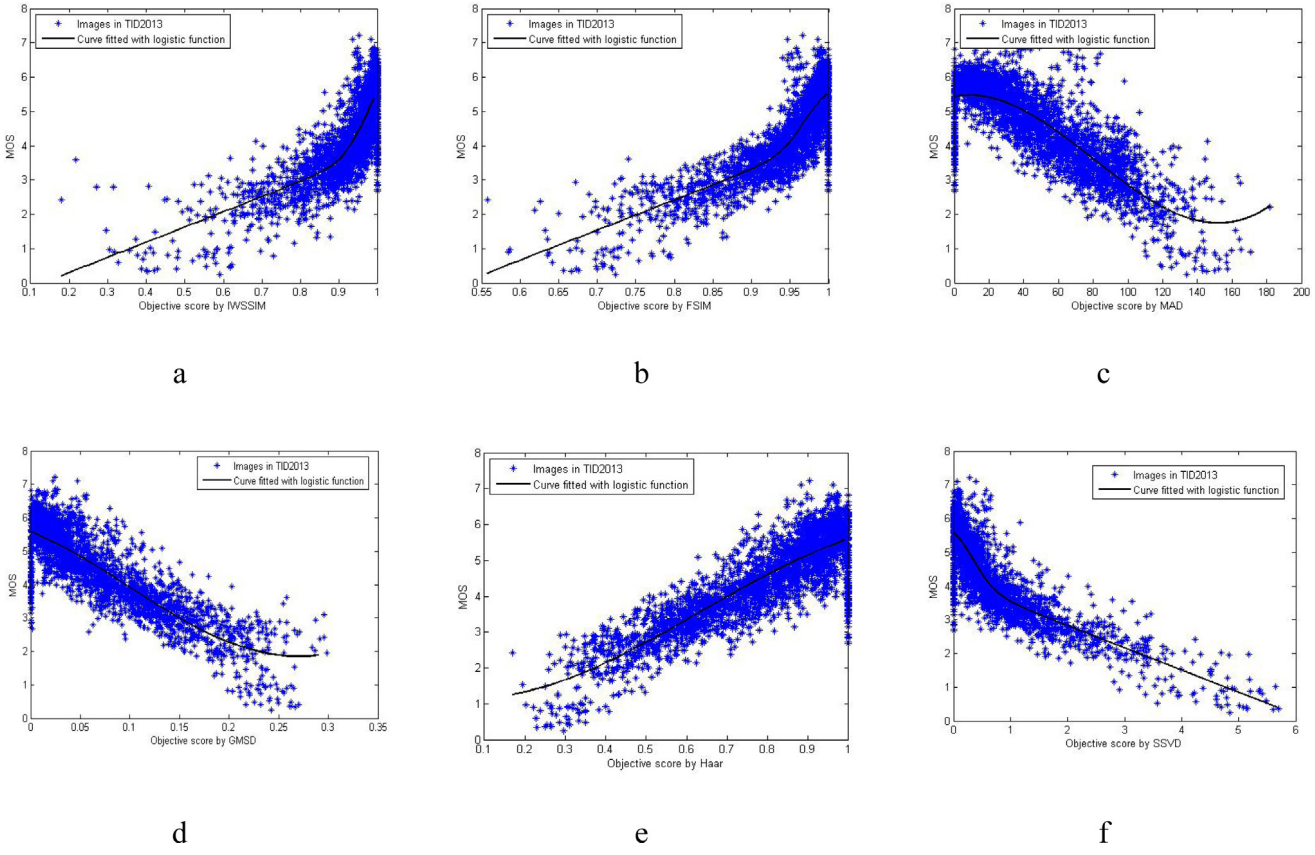

Fig. 7. Scatter plots of subjective MOS versus objective scores on the TID2013 dataset. (a) IWSSIM, (b) FSIM, (c) MAD, (d) GMSD, (e) HaarPSI, (f) SSVD (proposed method).

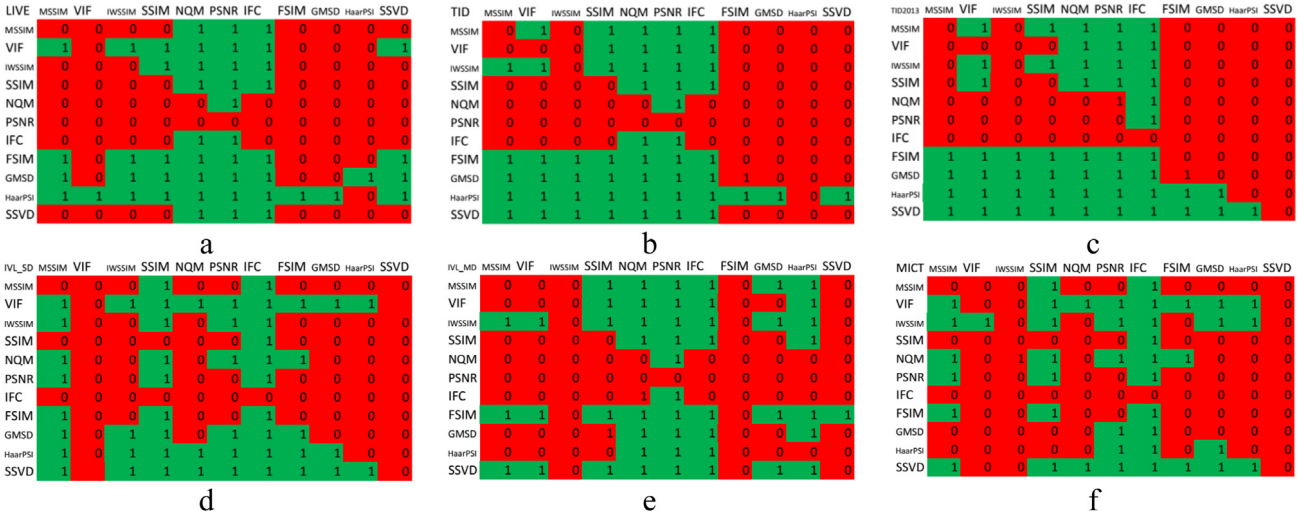

Fig. 8. The results of the statistical significance tests of the competing IQA methods on the — (a) LIVE, (b) TID2008 (c) TID2013 (d) IVL_SD (e) IVL_MD and (f) MICT databases. A value of '1' (highlighted in green) indicates that the method in the row is significantly better than the method in the column, while a value of '0' (highlighted in red) indicates that the first method is not significantly better than the second one.

especially in TID2013 and the multiply distorted dataset. Moreover, this experiment illustrates that the performance of some methods such as HaarPSI and GMSD can be highly affected by challenging datasets such as IVL.

Considering the experimental results illustrated in Table 2 and statistical significance tests depicted in Fig. 8, the performance of the state-of-art IQA methods are highly dependent on the dataset employed for evaluation. It can be concluded that finding a universal IQA method is still an open problem.

5. Conclusion

In this paper, a new full reference image quality metric based on singular value decomposition is proposed. The structural deformation of the distorted image is calculated by taking the advantages of its reflections on left and right original singular vectors. Furthermore, the difference between the singular values of the original image and the estimated singular values of the distorted image (reflected factor), are employed as a measure mostly representing the luminance distortion. Also, a regulating factor is introduced which reduces the effect of

Table 2
Performance of the proposed SSVD method and ten full-reference models in terms of SROCC, KROCC, PROCC, and RMSE on the ten databases.

		MSSIM	VIF	IWSSIM	SSIM	NQM	PSNR	IFC	FSIM	GMSD	Haar	SSVD
TID2013	SROCC	0.785	0.676	0.777	0.741	0.643	0.639	0.538	0.801	0.804	0.809	**0.811**
3000	KROCC	0.604	0.514	0.597	0.558	0.474	0.469	0.393	0.628	0.633	0.637	**0.647**
	PROCC	0.832	0.772	0.831	0.789	0.690	0.677	0.553	0.858	0.859	0.866	**0.872**
	RMSE	0.686	0.788	0.688	0.760	0.896	0.911	1.032	0.634	0.634	0.620	**0.608**
TID2008	SROCC	0.853	0.749	0.655	0.774	0.624	0.553	0.567	0.880	0.890	**0.905**	0.885
1700	KROCC	0.654	0.586	0.495	0.576	0.460	0.402	0.423	0.694	0.709	**0.727**	0.711
	PROCC	0.845	0.808	0.857	0.773	0.614	0.573	0.734	0.873	0.878	**0.901**	0.894
	RMSE	0.717	0.789	0.689	0.851	1.059	1.099	0.911	0.652	0.640	**0.583**	0.601
MICT	SROCC	0.887	0.907	**0.920**	0.879	0.891	0.613	0.835	0.905	0.852	0.882	0.910
168	KROCC	0.702	0.731	**0.753**	0.693	0.729	0.444	0.637	0.730	0.658	0.696	0.738
	PLCC	0.892	0.913	**0.924**	0.888	0.895	0.642	0.840	0.907	0.858	0.887	0.915
	RMSE	0.564	0.508	**0.476**	0.573	0.556	0.958	0.678	0.524	0.642	0.577	0.506
VCL	SROCC	0.922	0.886	0.916	0.911	**0.943**	0.824	0.857	0.917	0.917	0.922	0.933
552	KROCC	0.733	0.692	0.737	0.733	**0.781**	0.636	0.655	0.736	0.740	0.747	0.765
	PROCC	0.923	0.893	0.919	0.914	**0.942**	0.832	0.861	0.918	0.917	0.920	0.934
	RMSE	9.439	11.010	9.678	9.944	**8.178**	13.620	12.470	9.723	9.764	9.610	8.740
CSIQ	SROCC	0.913	0.919	0.921	0.875	0.740	0.805	0.767	0.924	**0.957**	0.955	0.898
866	KROCC	0.739	0.753	0.752	0.690	0.563	0.608	0.589	0.756	0.812	**0.813**	0.726
	PLCC	0.899	0.927	0.914	0.861	0.743	0.800	0.838	0.912	**0.954**	0.952	0.888
	RMSE	0.114	0.098	0.106	0.133	0.175	0.157	0.143	0.107	**0.078**	0.081	0.120
IVC	SROCC	0.898	0.896	0.912	0.901	0.834	0.688	0.899	0.926	0.914	0.921	**0.929**
185	KROCC	0.720	0.715	0.733	0.722	0.634	0.521	0.720	0.756	0.737	0.756	**0.761**
	PROCC	0.910	0.902	0.923	0.911	0.849	0.719	0.909	0.937	0.923	0.931	**0.935**
	RMSE	0.502	0.523	0.468	0.499	0.642	0.846	0.506	0.423	0.467	0.446	**0.431**
LIVE	SROCC	0.951	0.963	0.956	0.947	0.908	0.875	0.925	0.963	0.960	**0.969**	0.959
779	KROCC	0.804	0.828	0.817	0.796	0.741	0.686	0.757	0.833	0.826	**0.847**	0.819
	PROCC	0.948	0.960	0.952	0.944	0.912	0.872	0.926	0.959	0.960	**0.969**	0.956
	RMSE	8.618	7.613	8.347	8.945	11.190	13.350	10.260	7.678	7.621	**6.756**	8.060
WIQ	SROCC	0.749	0.691	0.786	0.726	0.764	0.625	0.715	0.800	0.798	**0.823**	0.795
80	KROCC	0.574	0.524	0.603	0.556	0.580	0.462	0.529	0.621	0.618	**0.641**	0.623
	PROCC	0.809	0.760	0.832	0.798	0.817	0.793	0.767	0.854	**0.873**	0.869	0.831
	RMSE	13.440	14.870	12.670	13.800	13.200	14.130	14.670	11.890	**11.130**	11.310	12.740
IVL_SD	SROCC	0.852	**0.937**	0.885	0.846	0.891	0.868	0.786	0.873	0.891	0.912	0.934
380	KROCC	0.642	**0.770**	0.680	0.636	0.699	0.683	0.581	0.671	0.692	0.723	0.766
	PROCC	0.858	**0.956**	0.895	0.852	0.906	0.874	0.791	0.888	0.907	0.931	**0.956**
	RMSE	12.107	**6.903**	10.536	12.358	9.982	11.469	14.456	10.839	9.951	8.605	6.947
IVL_MD	SROCC	0.827	0.838	**0.859**	0.797	0.746	0.614	0.781	0.859	0.821	0.814	**0.876**
750	KROCC	0.634	0.647	**0.671**	0.605	0.553	0.444	0.586	0.670	0.627	0.621	**0.689**
	PROCC	0.881	0.874	**0.906**	0.862	0.793	0.681	0.799	0.904	0.869	0.858	0.900
	RMSE	11.320	11.621	**10.129**	12.096	14.545	17.498	14.362	10.216	11.836	12.280	10.430
Weighted mean	AvSROCC	0.847	0.791	0.811	0.807	0.724	0.681	0.672	0.865	0.867	**0.875**	0.872
	AVKROCC	0.663	0.626	0.638	0.622	0.552	0.509	0.509	0.691	0.696	**0.706**	0.705
	AvPROCC	0.866	0.843	0.875	0.830	0.745	0.707	0.721	0.888	0.890	**0.899**	0.898
Mean	AvSROCC	0.864	0.846	0.859	0.840	0.798	0.710	0.767	0.885	0.880	0.891	**0.893**
	AVKROCC	0.681	0.676	0.684	0.656	0.621	0.535	0.587	0.709	0.705	0.721	**0.724**
	AvPROCC	0.880	0.876	0.895	0.859	0.816	0.746	0.802	0.901	0.900	**0.908**	**0.908**

luminance alterations in case of similar structures. Combining these factors provides an impressive image quality metric conforming HVS. The experimental results validate the effectiveness of the proposed method.

References

[1] Z. Wang, A.C. Bovik, L. Lu, Why is image quality assessment so difficult? in: Acoustics, Speech, and Signal Processing, ICASSP, 2002 IEEE International Conference on, 2002, pp. IV-3313–IV-3316.

[2] Z. Wang, A.C. Bovik, H.R. Sheikh, E.P. Simoncelli, Image quality assessment: From error visibility to structural similarity, IEEE Trans. Image Process. 13 (2004) 600–612.

[3] Z. Wang, A.C. Bovik, A universal image quality index, IEEE Signal Process. Lett. 9 (2002) 81–84.

[4] H.R. Sheikh, M.F. Sabir, A.C. Bovik, A statistical evaluation of recent full reference image quality assessment algorithms, IEEE Trans. Image Process. 15 (2006) 3440–3451.

[5] Z. Lin, D. Zhang, M. Xuanqin, D. Zhang, FSIM: A feature similarity index for image quality assessment, IEEE Trans. Image Process. 20 (2011) 2378–2386.

[6] A. Mahmoudi-Aznaveh, A. Mansouri, F. Torkamani-Azar, M. Eslami, Image quality measurement besides distortion type classifying, Opt. Rev. 16 (2009) 30–34.

[7] A. Mansouri, A. Mahmoudi-Aznaveh, F. Torkamani-Azar, J. Jahanshahi, Image quality assessment using the singular value decomposition theorem, Opt. Rev. 16 (2009) 49–53.

[8] M. Narwaria, L. Weisi, SVD-Based quality metric for image and video using machine learning, IEEE Trans. Syst. Man Cybern. B 42 (2012) 347–364.

[9] H.R. Sheikh, A.C. Bovik, G. de Veciana, An information fidelity criterion for image quality assessment using natural scene statistics, IEEE Trans. Image Process. 14 (2005) 2117–2128.

[10] Z. Wang, E.P. Simoncelli, A.C. Bovik, Multiscale structural similarity for image quality assessment, in: Signals, Systems and Computers, 2003 Conference Record of the Thirty-Seventh Asilomar Conference on, vol. 2, 2003, pp. 1398–1402.

[11] M.P. Sampat, Z. Wang, S. Gupta, A.C. Bovik, M.K. Markey, Complex wavelet structural similarity: A new image similarity index, IEEE Trans. Image Process. 18 (2009) 2385–2401.

[12] Z. Wang, Q. Li, Information content weighting for perceptual image quality assessment, IEEE Trans. Image Process. 20 (2011) 1185–1198.

[13] H.R. Sheikh, A.C. Bovik, Image information and visual quality, IEEE Trans. Image Process. 15 (2006) 430–444.

[14] A. Liu, W. Lin, M. Narwaria, Image quality assessment based on gradient similarity, IEEE Trans. Image Process. 21 (2012) 1500–1512.

[15] W. Sun, Q. Liao, J.H. Xue, F. Zhou, SPSIM: A superpixel-based similarity index for full-reference image quality assessment, IEEE Trans. Image Process. (2018) pp. 4232–4244.

[16] R. Reisenhofer, S. Bosse, G. Kutyniok, T. Wiegand, A haar wavelet-based perceptual similarity index for image quality assessment, Signal Process., Image Commun. 61 (2018) 33–43.
[17] A. Shnayderman, A. Gusev, A.M. Eskicioglu, An SVD-based grayscale image quality measure for local and global assessment, IEEE Trans. Image Process. 15 (2006) 422–429.
[18] M. Esmaeilpour, A. Mansouri, A. Mahmoudi-Aznaveh, A new SVD-based image quality assessment, in: Machine Vision and Image Processing, MVIP, 2013 8th Iranian Conference on, 2013, pp. 370–374.
[19] A. Hu, R. Zhang, D. Yin, Y. Zhan, Image quality assessment using a SVD-based structural projection, Signal Process., Image Commun. 29 (2014) 293–302.
[20] W. Shuigen, D. Chenwei, L. Weisi, Z. Baojun, C. Jie, A novel SVD-based image quality assessment metric, in: Image Processing, ICIP, 2013 20th IEEE International Conference on, 2013, pp. 423–426.
[21] M. Narwaria, L. Weisi, Objective image quality assessment based on support vector regression, IEEE Trans. Neural Netw. 21 (2010) 515–519.
[22] M. Narwaria, W. Lin, Scalable image quality assessment based on structural vectors, in: 2009 IEEE International Workshop on Multimedia Signal Processing, 2009, pp. 1–6.
[23] H. Andrews, C. Patterson, Singular value decompositions and digital image processing, IEEE Trans. Acoust. Speech Signal Process. 24 (1976) 26–53.
[24] K. Okarma, Combined full-reference image quality metric linearly correlated with subjective assessment, in: L. Rutkowski, R. Scherer, R. Tadeusiewicz, L. Zadeh, J. Zurada (Eds.), in: Artificial Intelligence and Soft Computing, vol. 6113, Springer Berlin Heidelberg, 2010, pp. 539–546.
[25] K. Okarma, Colour image quality assessment using the combined full-reference metric, in: Computer Recognition Systems 4, Berlin, Heidelberg, 2011, pp. 287–296.
[26] N. Ponomarenko, V. Lukin, A. Zelensky, K. Egiazarian, M. Carli, F. Battisti, TID2008-a database for evaluation of full-reference visual quality assessment metrics, Adv. Modern Radioelectron. 10 (2009) 30–45.
[27] N. Ponomarenko, L. Jin, O. Ieremeiev, V. Lukin, K. Egiazarian, J. Astola, et al., Image database TID2013: Peculiarities, results and perspectives, Signal Process., Image Commun. 30 (2015) 57–77.
[28] E.C. Larson, D.M. Chandler, Most apparent distortion: Full-reference image quality assessment and the role of strategy, J. Electron. Imaging 19 (2010) pp. 011006-011006-21.
[29] Y. Horita, K. Shibata, Y. Kawayoke, Z.P. Sazzad, MICT image quality evaluation database, [Online], http://mict.eng.u-toyama.ac.jp/mictdb.html, 2011.
[30] A. Zarić, N. Tatalović, N. Brajković, H. Hlevnjak, M. Lončarić, E. Dumić, et al., VCL@ FER image quality assessment database, AUTOMATIKA: časopis za automatiku, mjerenje, elektroniku, računarstvo i komunikacije 53 (2012) 344–354.
[31] A. Ninassi, P. Le Callet, F. Autrusseau, Subjective quality assessment-IVC database, [online] http://www.irccyn.ec-nantes.fr/ivcdb, 2006.
[32] U. Engelke, T. Kusuma, H. Zepernick, Wireless imaging quality (WIQ) database, ed, 2010.
[33] S. Corchs, F. Gasparini, R. Schettini, No reference image quality classification for JPEG-distorted images, Digit. Signal Process. 30 (2014) 86–100.
[34] S. Corchs, F. Gasparini, A Multidistortion Database for Image Quality, Cham, 2017, pp. 95–104.
[35] Z. Wang, SSIM Index for Image Quality Assessment Available: http://www.ece.uwaterloo.ca/~z70wang/research/ssim/, 2003.
[36] S.E. Palmer, Vision Science: Photons To Phenomenology, MIT press, 1999.
[37] W. Xue, L. Zhang, X. Mou, A.C. Bovik, Gradient magnitude similarity deviation: A highly efficient perceptual image quality index, IEEE Trans. Image Process. 23 (2014) 684–695.
[38] R. Zhu, F. Zhou, W. Yang, J. Xue, On hypothesis testing for comparing image quality assessment metrics [tips & tricks], IEEE Signal Process. Mag. 35 (2018) 133–136.